Trans. Phenom. Nano Micro Scales, 1(1): 53-63, Winter - Spring 2013
DOI: 10.7508/tpnms.2013.01.006

ORIGINAL RESEARCH PAPER

Study on Thermal and Hydrodynamic Indexes of a Nanofluid Flow in a Micro Heat Sink

M. Izadi[1,*] , M. M. Shahmardan [1], A. M. Rashidi[2]
[1]*Mechanical Engineering Department, Shahrood University of Technology, Shahrood, Iran*
[2]*Nanotechnology Research Center, Research Institute of Petroleum Industry (R.I.P.I)*

Abstract

The paper numerically presents laminar forced convection of a nanofluid flowing in a duct at microscale. Results were compared with both analytical and experimental data and observed good concordance with previous studies available in the literature. Influences of Brinkman and Reynolds number on thermal and hydrodynamic indexes have been investigated. For a given nanofluid, no change in efficiency (heat dissipation to pumping power) was observed with an increasing in Reynolds number. It was shown that the pressure was decrease with an increase in Brinkman number. Dependency of Nu increment changes with substrate material.

Keywords: *Microchannel heat sink; Nanofluid; Viscous dissipation effect*

1. Introduction

In recent years, development in the miniaturization technologies results in fabrication of micro-scale electronic devices which is used in various industries such as aerospace and automotive. For maximum performance of these micro devices which is known as MEMS (Micro Electromechanical Systems), the temperatures should be in a certain range. Microchannel [1] as Compact and efficient cooling devices have been developed for the thermal control of MEMS. Utilizing nanofluid as working fluid could improve the cooling performance of microchannel. Because of more stable nature of nanofluid compared with its pioneer generation (including micro and millimeter particles) and exceptional thermal conductivity of nanoparticles, it could considerably enhance the convective heat transfer coefficient in microchannel.

During the last decade, many studies on convective heat transfer with nanofluids have been considered [2-6]. Pak and Cho [2] revealed that the heat transfer coefficients of the nanofluids increase with increasing the volume fraction of nanoparticles and the Reynolds number. Mirmasoumi and Behzadmehr [7] studied the laminar mixed convection of an Al_2O_3/water nanofluid in a horizontal tube numerically using a two-phase mixture model. They showed that the nanoparticle concentration did not have significant effects on the hydrodynamics parameters, but its effects on the thermal parameters were important for the fully developed region. Izadi et al. [8] considered the laminar forced convection of an Al_2O_3 /water nanofluid flowing in an annulus. Their results indicate that the friction coefficient depends on the nanoparticle concentration when the order of magnitude of heating energy is much higher than the momentum energy.

Thermal transport of nanofluid flow in microchannels has also attracted a few investigators [9-15] due to its promising applications. In a study by Jang et al [11] the cooling performance of the

[*]Corresponding author
Email Address: m.izadi.mec@gmail.com

Nomenclature

C	Specific heat (J/kg K)		**Index**
d	diameter	0	inlet condition
d_{bf}	Molecular diameter of base fluid (nm)	a	average
d_h	hydraulic diameter, µm	bf	base fluid
d_p	Nanoparticle diameter (nm)	ch	microchannel
h	Nanoparticle diameter (nm)	d	down
h_{ch}	heat transfer coefficient, (W/m^2 K)	eff	effective
k	channel height, µm	fr	freezing point
k_b	Boltzmann's constant (J/K)	h	hydraulic
K_b	Boltzmann's constant	i,j	indexes
M	molecular weight of the base fluid	nf	nanofluid
N	Avogadro number	o	outer
Nu	Nusselt number	p	particle
P	Pressure (Pa)	s	solid substrate
pr	Prandtl number	u	upper
q	heat flux	w	wall
t (t_{d+} t_u+h_{ch})	total height of channel, µm		**Greek**
t	MCHS wall thickness, µm	µ	Dynamic viscosity (N s/m^2)
T	Temperature (K)	β	performance index
t_d	MCHS upper wall thickness, µm	ε	strain rate tensor
t_u	MCHS upper wall thickness, µm	ρ	Density (kg/m^3)
u	velocity, m/s	τ	stress (pa)
x, y	axial and cross section direction, m	φ	Nanoparticle volume fraction

microchannel was significantly improved by the significant reduction in the temperature difference between the heated wall and the nanofluids. Ho et al. [12] experimentally assessed forced convective cooling performance of a copper microchannel heat sink with Al_2O_3/water nanofluid as a coolant. Their Results show that the nanofluid cooled heat sink outperforms the water-cooled one, having significantly higher average heat transfer coefficient and thereby markedly lower thermal resistance and wall temperature at high pumping power, in particular. Meanwhile, in an experiment [14] using SiO_2–water nanofluids in a aluminum heat sink consisted of an array of 4 mm diameter circular channels with a length of 40 mm. The experimental results showed that dispersing SiO_2 nanoparticles in water significantly increased the overall heat transfer coefficient while thermal resistance of heat sink was decreased up to 10%.Also they numerically investigated corresponding configuration. The results revealed that channel diameter, as well as heat sink height and number of channels in a heat sink have significant effects on the maximum temperature of heat sink.

Regarding numerical aspects, Kosar [16] demonstrated when the commonly used assumption of constant heat flux boundary condition is applicable in heat and fluid flow analysis in microfluidic systems. Also a general Nusselt number correlation for fully developed laminar flow was developed as a function of two dimensionless parameters, namely, Biot number and relative

conductivity, to take the Conduction effects of the solid substrate on heat transfer into account. Kalteh et al. [17] numerically and experimentally studied the thermal characteristics of an alumina-water nanofluid flow inside a wide rectangular microchannel. In their study, a two-phase method was adopted. Their comparison shows that two-phase modeling results have better concordance with experimental data than the homogeneous (single-phase) approach.

Few researches on characteristics of nanofluids which experimentally behave as non-Newtonian have been performed. For example Hojjat et al. [18] prepared three kinds of nanofluids by dispersing g-Al_2O_3, CuO, and TiO_2 nanoparticles in asolution of carboxymethyl cellulose (CMC). They proposed a new correlation to predict successfully the Nusselt number of non-Newtonian nanofluids as a function of the Reynolds and the Prandtl numbers.

In most of the cases, heat transfer in microchannels is connected with conduction effects of substrate. Most of researches are performed Regardless the substrate material and thickness under the assumption of constant heat flux boundary condition. For cases where thick and low thermal conductivity (such as polymers) substrates are utilized commonly used constant heat flux boundary condition may not be valid. Thus many researchers have been performed studies on single-phase flow in micro-heat sinks to investigate their thermal performances and the conjugate effects [19].

This paper aims to consider conjugate conduction and convection heat transfer of nanofluids flow in a deep of rectangular (parallel plate) microchannel with assumption constant heat flux boundary condition.

According to the literature [20–25], in microscale systems, large channel length to hydraulic diameter ratios brings about large velocity and as a result thermal energy generation due to viscous dissipation effects. Thus, this paper studied some attributes of nanofluids flow performane in above described configuration.

2. Mathematical modeling

This section describes the mathematical formulation of the problem. The constant wall heat flux (H) was considered as thermal boundary conditions. It covers the effect of brinkman number on laminar forced convection of nanofluid flowing between two parallel plates (wide rectangular cross section). The problem which was considered is depicted schematically in Fig. 1. A wide rectangular microchannel (high width to height) permits that the computational domain of solution restricts to two dimensions. Corcione [26] proposed a correlation were used to calculate the effective viscosity and thermal conductivity of nanofluid. To focus on the effect on the heat sink performance due to the brinkman number, following assumptions were made:

(1) Both nanofluid flow and heat transfer are in steady-state and two dimensions.

(2) nanofluid is in single phase and flow is laminar.

(3) All the surfaces of heat sink are cooled by the surroundings.

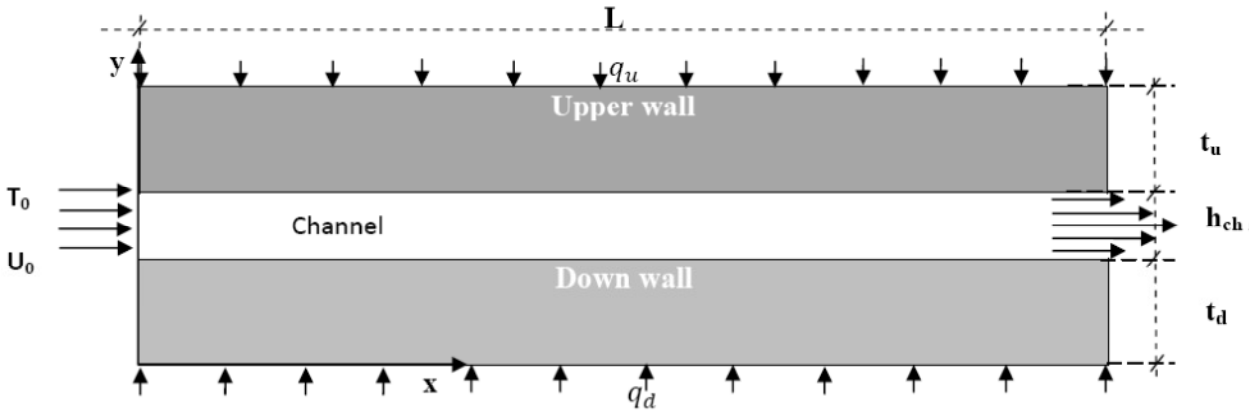

Fig1. Geometric configuration of microchannel heat sink.

3. Governing equations

The continuity, momentum and energy equations for the problem can be written in Cartesian tensor notation as

Continuity equation

$$\frac{\partial}{\partial x_i}(\rho u_i)=0 \quad (1)$$

Momentum equation

According to above mentioned assumption, Momentum equation in Cartesian coordinates takes the following general form [30]:

$$\frac{\partial}{\partial x_i}\left(\rho u_j u_i\right)=\frac{\partial \tau_{ij}}{\partial x_i} \quad (2)$$

Where $\tau_{ij}=-P\delta_{ij}+2\mu\varepsilon_{ij}$ $\varepsilon_{ij}=\frac{1}{2}\left(\frac{\partial u_i}{\partial x_j}+\frac{\partial u_j}{\partial x_i}\right)$

Where ε_{ij}, P and μ are strain tensor, pressure and viscosity, respectively.

Energy equation:

$$\frac{\partial}{\partial x_i}(\rho c T u_i)=\frac{\partial q_i}{\partial x_i}+\tau_{ij}\varepsilon_{ij} \quad (3)$$

The term of $\tau_{ij}\varepsilon_{ij}$ is Deformation work ($=-P\varepsilon_{ii}+2\mu\varepsilon_{ij}:\varepsilon_{ij}$, rate per volume) that for incompressible flow, the first term in right hand side of equation is zero.

3.1. Boundary condition:

The following boundary condition was set to solve the set of governing equation:

- At flow inlet: Uniform velocity and temperature ($T=T_0$, $u=u_0$ and $v=0$)
- At the flow outlet: fully developed condition was adapted for momentum. Input and output energy were balanced for energy equation.
- At nanofluid-solid interface:

1) At inner side of walls: $T_s=T_{nf}$ and
2) $k_s\left(\frac{\partial T}{\partial y}\right)_s=k_{eff}\left(\frac{\partial T}{\partial y}\right)_{nf}$, u=0 and v=0.
3) at inlet and outlet: $\left(\frac{\partial T}{\partial x}\right)_s=0$

- At outer side of walls: y=0 and y=h $q=k_s\left(\frac{\partial T}{\partial x}\right)_s$

4. Physical properties of nanofluid

4.1. Effective thermal conductivity

An Empirical correlation proposed Corcione [26] was used for calculating the effective thermal conductivity:

$$\frac{k_{eff}}{k_{bf}}=1+4.4Re^{0.4}Pr_{bf}^{0.66}\left(\frac{T}{T_{fr}}\right)^{10}\left(\frac{k_p}{k_{bf}}\right)^{0.03}\varphi^{0.66}$$

Where $Re=\frac{2\rho_{bf}k_bT}{\pi\mu_{bf}^2d_p}$ is the nanoparticle Reynolds number.

For more detail of the correlation, one could refer to reference [26].

4.2. Effective dynamic viscosity

Corcione [26] also presented a correlation for prediction of effective dynamic viscosity which was derived from a wide-ranging of experimental data available in the literature. This empirical correlation was utilized to calculate effective dynamic viscosity.

$$\frac{\mu_{eff}}{\mu_{bf}}=\frac{1}{1-34.87\left(d_p/d_{bf}\right)^{-0.3}\varphi^{1.03}}$$

Where $d=\left(\frac{6M}{N\pi\rho_{f0}}\right)^{1/3}$

Reference [26] presents comprehensive information about above effective dynamic viscosity.

The physical properties are the following:

4.3. Effective density:

$$\rho_{eff}=(1-\phi)\rho_f+\phi\rho_p \quad (4)$$

4.4. Effective specific heat:

To calculate the effective heat capacity of nanofluid, an accurate relation given by (Putra et al, 2003) is used.

$$C_{eff}=\frac{(1-\phi)\rho_f C_f+\phi\rho_p C_p}{\rho_{eff}} \quad (5)$$

Dimensionless parameters were defined as follow:

Reynolds number: $Re=\frac{\rho_{eff}u_0d_h}{\mu_{eff}}$

Brinkman number: the Brinkman number represents the relationship between viscosity and velocity in the presence of heat transfer ($Br=\frac{\mu_{eff}{u_0}^2}{qd_h}$).

5. Numerical method:

The triple governing equations (equations 1-3) were solved by the SIMPLE algorithm, a finite volume technique. The grids were refined near the wall and entrance region where the variable gradient is high to obtain highly accurate numerical result. To evaluate the grid independent test as shown in fig. 2, the grid size was fined until acceptable grid size was found. The selected grid for the present study consists of 200 and 132 nodes respectively in the axial and cross directions. As seen in Fig. 1 that no change is observed in the thermal and hydrodynamic results up to previous grid number.

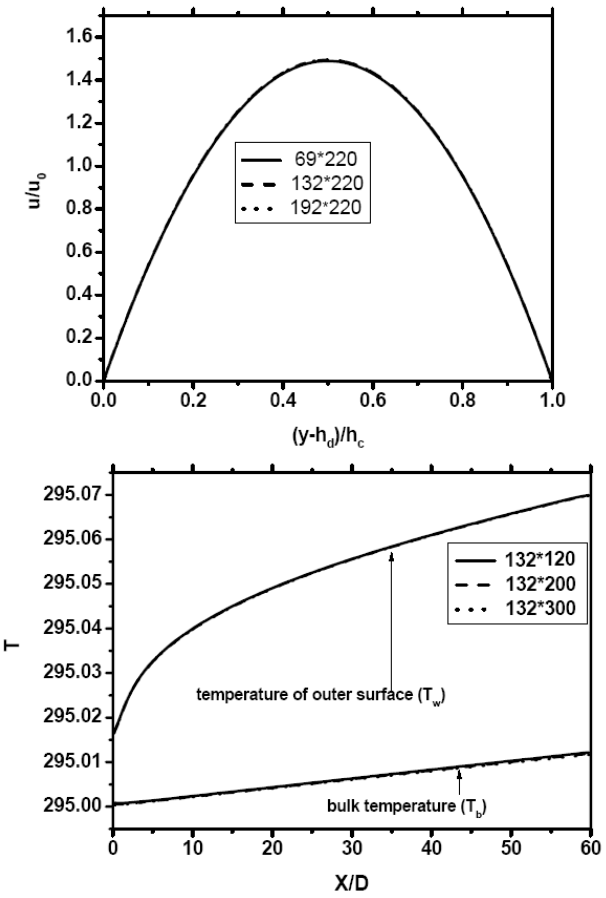

Fig. 2. Grid independence tests

6. Code validation

The accuracy of the homemade code was verified by comparing the results with available corresponding analytical and experimental data. As shown in Fig. 3, dimensionless axial velocity of base fluid (φ=0) has good agreement with corresponding analytical data [28]. Also, for pure water, table 1 performs a comparison between present code and analytical correlation available in the literatures [28] at different boundary condition (contrasting ratio of heat flux imposed on walls). Fig. 3 displayed that a adapted comparison with recent experimental work of Kalteh et al. [29]. Therefore, numerical code is credible to predict the thermal and hydrodynamic behavior of a nanofluid flow in a micro heat sink.

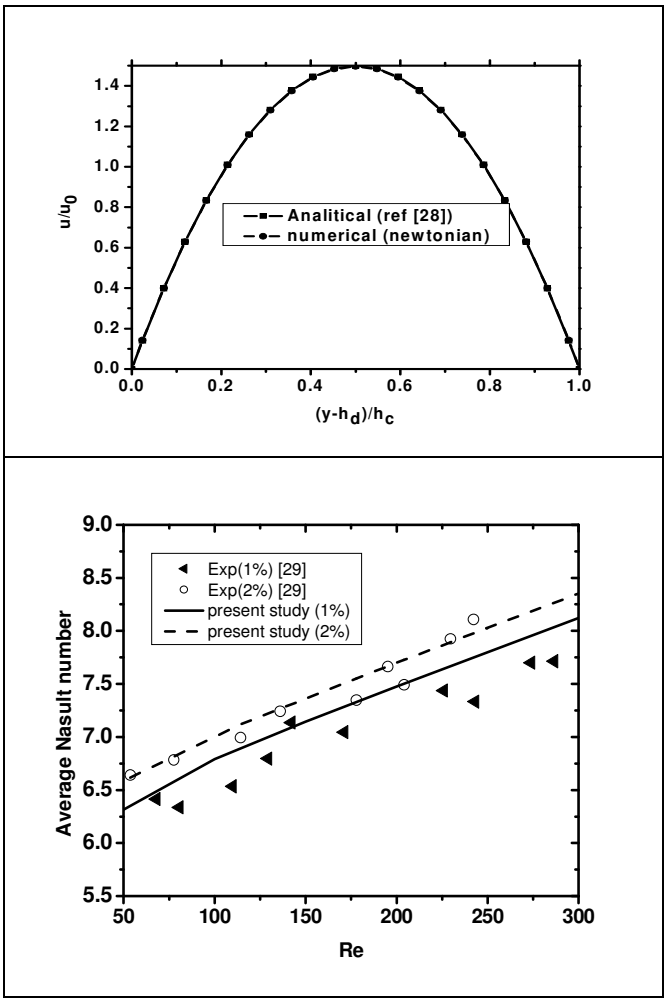

Fig. 3 comparison with the experimental results (a) analytical solution [28].(b) experimental data [29].

7. Result and discussion

Effect of Brinkman and Reynolds number, substrate material on cooling performance of Al_3O_2–water nanofluid throughout a heat sink microchannel was studied numerically. The calculations were done with Brinkman number identical at opposite plates of

the heat sink. Also material and thickness of two parallel plates were same. Brinkman number which is defined as $Br=\mu u_0^2/(qd_h)$ represents the relationship between viscosity and velocity in the presence of heat transfer. Local heat transfer coefficient and local Nusselt number were calculated using the following equations:

$$h = \frac{q}{T_w - T_b}$$

$$Nu = \frac{hd_h}{k_{\text{eff}}}$$

Where q, d_h, k_{eff}, T_w and T_b are heat flux, hydraulic diameter, effective thermal conductivity of the nanofluid fluid, wall temperature and bulk temperature across the heat sink. An important parameter in the MCHS operation is the coolant pumping power which relates to the pressure drop across the MCHS.

Table 1. Comparison of the present Nusselt number with the corresponding analytical solution [28].

Nu			
q_d/q_u	numerical	analytical	error(%)
0.25	6.2522	5.8947	6.06477
0.5	6.8120	6.5116	4.61331
0.65	7.2010	6.9479	3.64283
0.9	7.9633	7.8212	1.81686
1	8.3173	8.2353	0.99571
1.1	8.7054	8.6957	0.11155
1.25	**9.3631**	9.4915	1.35279

Table 2 consists of data of total pressure drop for different Reynolds number. Pressure drop increment has remarkable value when concentration of nanoparticles in nanofluid is increased. However, Wall material has no impact on Pressure drop increment while Reynolds number slightly decreases it from φ=2% to φ=6%.

Table 2
Total Pressure drop at different Reynolds number

	Total Pressure drop (Δp)					
	Pyrex (K=1.1)			Aluminum(K=237)		
Re	φ=2%	φ=6%	Increase %	φ=2%	φ=6%	Increase %
100	368.13597	866.82934	135.46445	368.13221	866.8116	135.46204
300	1128.1808	2647.8556	134.70135	1128.162	2647.7885	134.69932
600	2323.6181	5415.2051	133.05056	2323.571	5415.0803	133.04992
900	3581.1524	8274.1159	131.04618	3581.0909	8274.0206	131.04749
1200	4896.7361	11204.284	128.81127	4896.6684	11204.344	128.81566

Table 3
Total Nusselt number at different Reynolds number.

	Total Nusselt number (Nu)					
	Pyrex (K=1.1)			Aluminum(K=237)		
Re	φ=2%	φ=6%	Increase %	φ=2%	φ=6%	Increase %
100	1.9365	1.963	1.36793	5.40042	6.2438	15.6169
300	2.19133	2.16458	-1.22059	7.83764	8.80311	12.31845
600	2.3132	2.27352	-1.71534	9.69663	10.97156	13.14812
900	2.38259	2.33689	-1.91836	11.0759	12.62703	14.00452
1200	2.43171	2.38184	-2.0509	12.23867	14.04369	14.74848

Table 3. Shows that for a given Brinkman number and low thermal conductivity wall (Pyrex), Nu increment is low at Re=100. In a given Brinkman number, q (dissipated heat) is increased with φ. Under such situation, the temperature of Pyrex could remarkably increases. Thus such behavior decreases the Nu increment. For a given Br, This behavior intensifies in high Reynolds number and then high q value. For aluminum substrate with high thermal conductivity, such behavior would be weak. Although Nu increases with φ, Nu increment has not a distinct behavior with Re. At the beginning it decreases from 100 up to 300 and then increases up to 1200. But two previous parameters don't seem to be a suitable performance indexes. A performance index which is defined as the ratio of heat transferred between the fluids to total pumping power ($\beta = \frac{q}{p_{pump}}$) was used to show efficiency of microchannel with fixed Br. This ratio indicates the desirable cooling indicator (heat which dissipated) to cost operating condition. Table 4. Present data for β under similar condition with Br constant. For two wall materials, β increment is positive with an increase in φ. It intensifies when wall makes from a material with higher thermal conductivity (Aluminum). Also for a wall material, at the high value of Reynolds number the indicator growth is more significant. Because, for a given Brinkman number, at the high value of Reynolds number the augmentation of dissipation heat is farther than pumping power.

Fig. 4 shows the velocity profiles at fully developed region and two Re (100 and 1200). According to the figure, for Re=100, the velocity profile is not affected by Changing in brinkman number. In the other hand for Re=1200, Brinkman number has remarkable effects on the axial velocity. This arises from the fact that at high Reynolds number, decreasing in Brinkman number could significantly augment the dissipation heat and subsequently change the temperature of nanofluid flow which affects the viscosity of the fluid.

Table 4
Performance index at different Reynolds number

	performance index ($\beta = \frac{q}{p_{pump}}$)					
	Pyrex (K=1.1)			Aluminum(K=237)		
Re	φ=2%	φ=6%	Increase %	φ=2%	φ=6%	Increase %
100	415.26977	415.62506	0.08556	415.27401	415.63356	0.08658
300	406.51927	408.18992	0.41096	406.52604	408.20027	0.41184
600	394.75267	399.18265	1.12222	394.76066	399.19186	1.1225
900	384.20081	391.88283	1.99948	384.2074	391.88734	1.9989
1200	374.63911	385.8624	2.99576	374.6443	385.86034	2.99378

Fig. 5 displays the effect of Brinkman number on average Nu for microchannels of the same size and substrate thickness. Nu decreases with an increasing in Brinkman number. For high Brinkman number, average Nusselt numbers converge to a certain value. The average Nusselt number is affected by substrate material at low value of Br more than high value. However, when the order of magnitude of thermal diffusion term is much higher than the viscous dissipation term Nu depends on the substrate material. At higher Brinkman numbers for which the thermal diffusion decreases, this dependency on the substrate material decreases.

For two Reynolds number100 and 1200, the effect of Brinkman number on the pressure is, respectively, represented in Figs. 6. At low Reynolds number (100), the Brinkman number is not impressive on the axial evolution of pressure. While at high Reynolds number, it is affected appreciably for φ=2% ($Br<2*10^{-4}$) and φ=6% ($Br<2*10^{-3}$). This phenomenon is found to be more pronounced with inclusion of more nanoparticles (φ=6%). Because at the high value of Reynolds number the variation of fluid temperature along the microchannel length as a function of Brinkman number are significant and it could influence the variation of viscosity

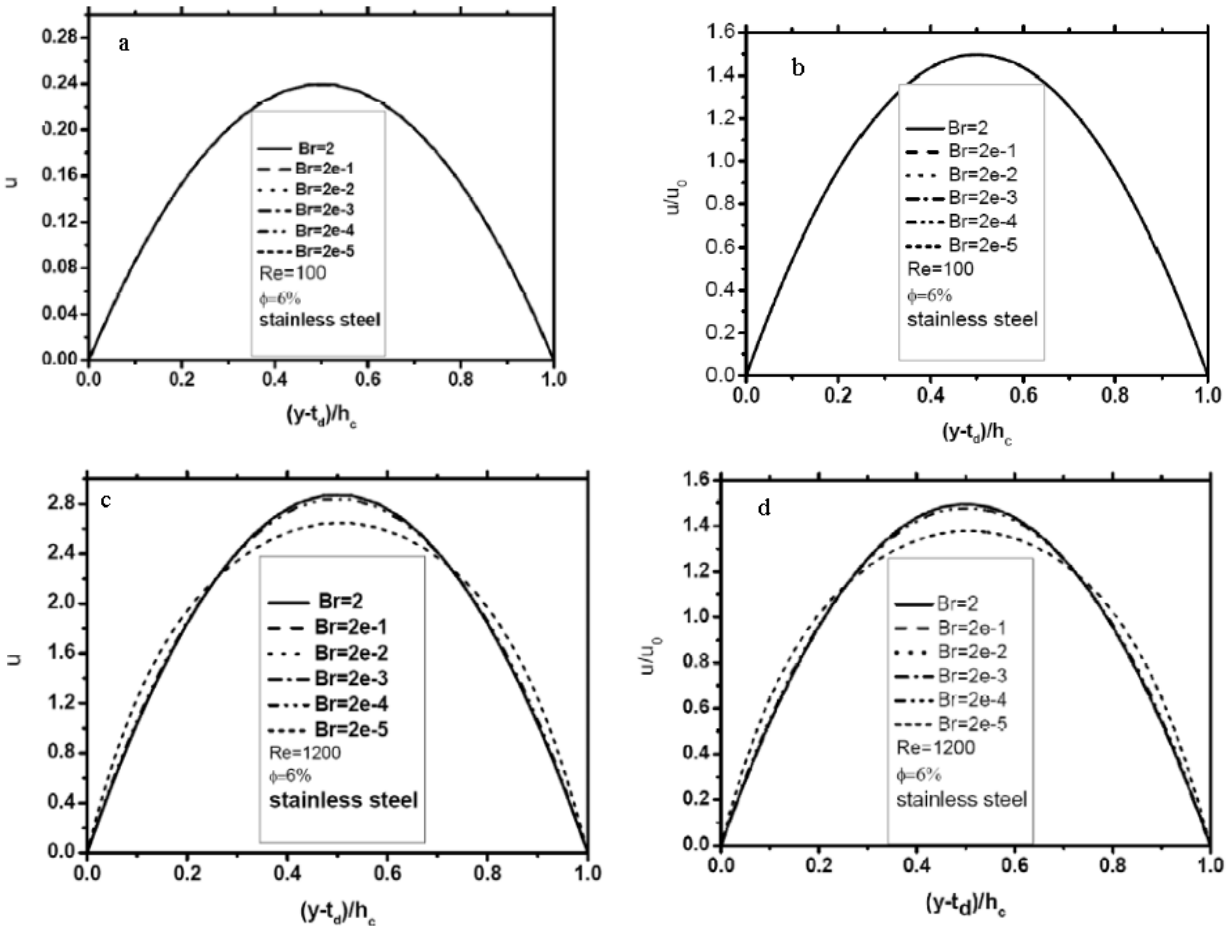

Fig. 4 Dimensional and dimensionless fully developed velocity profile.

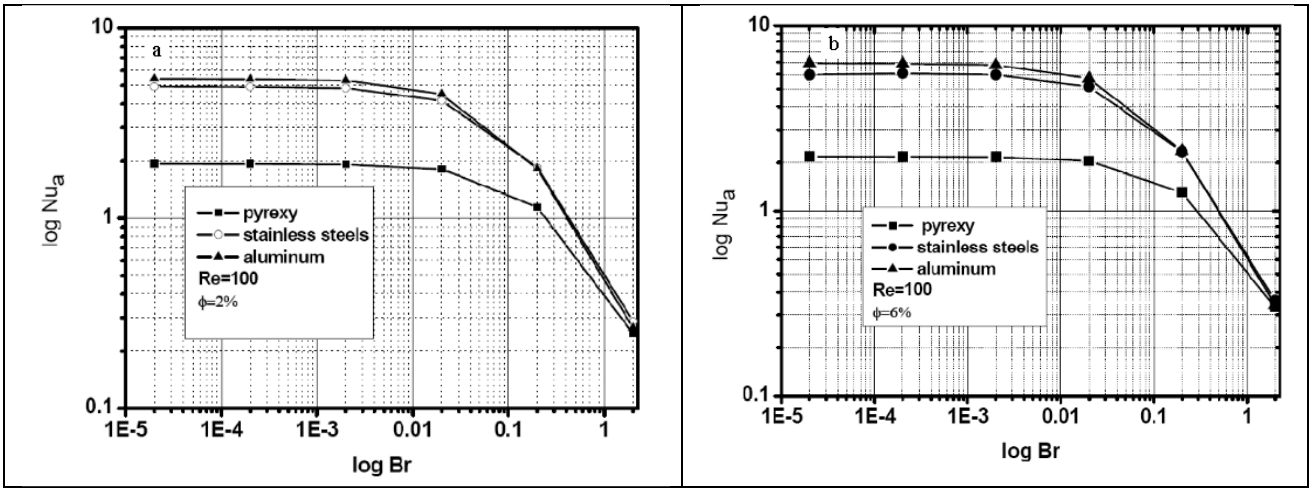

Fig. 5. Logarithmic variation of Nusselt numbers versus Brinkman number.

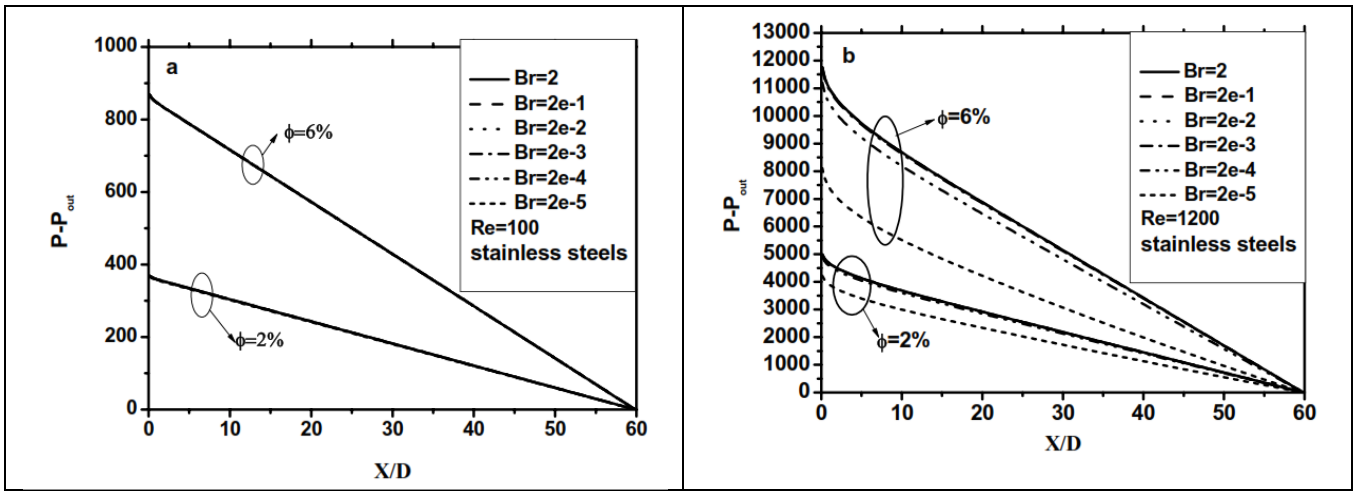

Fig. 6. Axial evolution of pressure for different Brinkman number.

(viscosity consider as a function of temperature). The latter is the reason for important variation of pressure at the high Reynolds number.

Fig. 7 shows Performance index (β) at different values of the Brinkman numbers for two different Reynolds numbers. Increasing the Brinkman numbers decreases the β at such conditions.

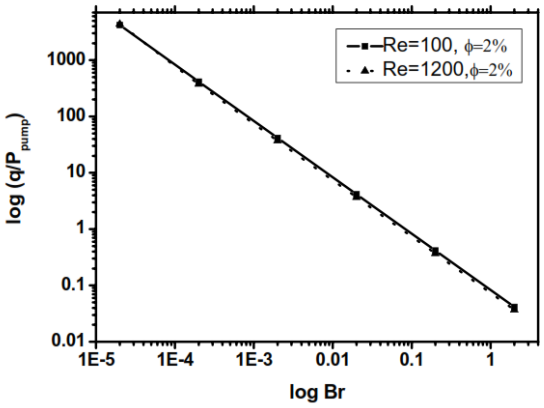

Fig. 7. Logarithmic variation of Performance index versus Brinkman number.

8. Conclusion

Forced convection of a nanofluid flowing in microchannel has been studied numerically. The results could be summarized at the following items:

- Wall material has no impact on Pressure drop increment while Reynolds number slightly decreases it from φ=2% to φ=6%.
- Although Nu increases with φ, Nu increment has not a distinct behavior with Re.
- At the high value of Reynolds number, the β growth is more significant Because of augmentation of dissipation heat.
- Dependency of Nu on the substrate material decreases decreases at higher Brinkman numbers for which the thermal diffusion decreases.

References

[1] D.B. Tuckerman, R.F.W. Pease, High performance heat sinking for VLSI, IEEE Electron. Devices Lett. EDL-2 (5) (1981) 126–129.

[2] B.C. Pak, Y.I. Cho, Hydrodynamic and heat transfer study of dispersed fluids with submicron metallic oxide particles, Exp. Heat Transfer 11 (1998) 151–170.

[3] S. Lee, S.U.S. Choi, Applications of metallic nanoparticle suspensions in advanced cooling system, in: Y Kwon, D.C. Davis, H.H. Chung (Eds.), Recent Advances in Solid/Structures and Application of Metallic Materials, PVP-vol. 342/MD-vol. 72, ASME, New York, 1996, pp. 227–234.

[4] Y. Xuan, Q. Li, Investigation on convective heat transfer and flow features of nanofluids, ASME J. Heat Transfer 125 (2003) 151–155.

[5] D. Wen, Y. Ding, Experimental investigation into convective heat transfer of nanofluids at the entrance region under laminar flow conditions, Int. J. Heat Mass Transfer 47 (2004) 5181–5188.

[6] J. Buongiorno, Convective transport in nanofluids, ASME J. Heat Transfer 128 (2006) 240–250.

[7] Mirmasoumi, S., Behzadmehr, A., Numerical study of laminar mixed convection of a nanofluid in a horizontal tube using two-phase mixture model, Applied Applied Thermal Engineering 28 2008; 717–727.

[8] Izadi, M., Behzadmehr A., Jalali-Vahid, D., Numerical study of developing laminar forced convection of a nanofluid in an annulus, International Journal of Thermal Sciences 48 2009; 2119–2129.

[9] R. Chein, J. Chuang,Experimental microchannel heat sink performance studies using nanofluids, International Journal of Thermal Sciences 46 (2007) 57–66.

[10] R. Chein, J. Chuang, Experimental microchannel heat sink performance studies using nanofluids, International Journal of Thermal Sciences 46 (2007) 57–66.

[11] J. Y. Jung, H. S. Oh, H.Y. Kwak, Forced convective heat transfer of nanofluids in microchannels, International Journal of Heat and Mass Transfer 52 (2009) 466–472.

[12] C.J. Ho, L.C. We, Z.W. Li, An experimental investigation of forced convective cooling performance of a microchannel heat sink with Al2O3/water nanofluid, Applied Thermal Engineering 30 (2010) 96-103.

[13] M. D. Byrne, R. A. Hart, A. K. da Silva, Experimental thermal–hydraulic evaluation of CuO nanofluids in microchannels at various concentrations with and without suspension enhancers, International Journal of Heat and Mass Transfer 55 (2012) 2684-2692.

[14] S. A. Fazeli, S. M. Hosseini Hashemi, H. Zirakzadeh, M. Ashjaee, Experimental and numerical investigation of heat transfer in a miniature heat sink utilizing silica nanofluid, Superlattices and Microstructures 51 (2012) 247–264.

[15] M. Kalteh, A. Abbassi , M Saffar-Avval, A. Frijns, A. Darhuber, J. Harting, Experimental and numerical investigation of nanofluid forced convection inside a wide microchannel heat sink, Applied Thermal Engineering 36 (2012) 260-268.

[16] Kosar, Effect of substrate thickness and material on heat transfer in microchannel heat sinks, International Journal of Thermal Sciences 49 (2010) 635-642.

[17] M. Kalteh, A. Abbassi, M Saffar-Avval, Jens Harting, Eulerian–Eulerian two-phase numerical simulation of nanofluid laminar forced convection in a microchannel, International Journal of Heat and Fluid Flow 32 (2011) 107-116.

[18] M. Hojjat , S.Gh. Etemad , R. Bagheri , J. Thibault, Rheological characteristics of non-Newtonian nanofluids: Experimental investigation, International Communications in Heat and Mass Transfer 38 (2011) 144–148.

[19] A.G. Fedorov, R. Viskanta, Three dimensional conjugate heat transfer in the microchannel heat sink for electronic packaging. International Journal of Heat

[20] and Mass Transfer 43 (2000) 399e415.

[21] G. Tunc, Y. Bayazitoglu, Heat transfer in microtubes with viscous dissipation, Int. J. Heat Mass Transfer 44 (2001) 2395–2403.

[22] H.-E. Jeong, J.-T. Jeong, Extended Graetz problem including streamwise conduction and viscous dissipation in microchannel, International Journal of Heat and Mass Transfer 49 (2006) 2151–2157.

[23] P.M. Coelho, F.T. Pinho, Fully-developed heat transfer in annuli with viscous dissipation, Int. J. Heat Mass Transfer 49 (2006) 3349–3359.

[24] S. Del Giudice, C. Nonino, S. Savino, Effects of viscous dissipation and temperature dependent viscosity in thermally and simultaneously developing laminar flows in microchannels, Int. J. Heat Fluid Flow 28 (2007) 15–27.

[25] O. Aydin, M. Avci, Analysis of laminar heat transfer in micro-Poiseuille flow, International Journal of Thermal Sciences 46 (2007) 30–37.

[26] K. Hooman, Entropy generation for microscale forced convection: Effects of different thermal boundary conditions, velocity slip, temperature jump, viscous dissipation, and duct geometry, International Communications in Heat and Mass Transfer 34 (2007) 945–957.

[27] M. Corcione, Empirical correlating equations for predicting the effective thermal conductivity and dynamic viscosity of nanofluids, Energy Conversion and Management 52 (2011) 789-793.

[28] T. X. Phuoc, M. Massoudi, R. Chen, Viscosity and thermal conductivity of nanofluids containing multi-walled carbon nanotubes stabilized by chitosan, International Journal of Thermal Sciences 50 (2011) 12-18.

[29] Ebadian, M.A., Dong, Z.F., 1998. Forced convection, internal flow in ducts. In: Rohsenow, W.M., Hartnett, J.P., Cho, Y.I. (Eds.), Handbook of Heat Transfer.McGraw-Hill, New York, pp. 5.1–5.137.

[30] M. Kalteh, A. Abbassi , M Saffar-Avval, A. Frijns, A. Darhuber, J. Harting, Experimental and numerical investigation of nanofluid forced

convection inside a wide microchannel heat sink, Applied Thermal Engineering 36 (2012) 260-268.
[31] M.B. Abbott and D.R. Basco, Computational fluid dynamics: An introduction for engineers, Longman Scientific & Technical, 1989.